

ORIGINAL ARTICLE

Open Access

Metabolic and microbial community dynamics during the hydrolytic and acidogenic fermentation in a leach-bed process

Heike Sträuber^{1,2*}, Martina Schröder¹ and Sabine Kleinsteuber^{1,2}

Abstract

Background: Biogas production from lignocellulosic feedstock not competing with food production can contribute to a sustainable bioenergy system. The hydrolysis is the rate-limiting step in the anaerobic digestion of solid substrates such as straw. Hence, a detailed understanding of the metabolic processes during the steps of hydrolysis and acidogenesis is required to improve process control strategies.

Methods: The fermentation products formed during the acidogenic fermentation of maize silage as a model substrate in a leach-bed process were determined by gas and liquid chromatography. The bacterial community dynamics was monitored by terminal restriction fragment length polymorphism analysis. The community profiles were correlated with the process data using multivariate statistics.

Results: The batch process comprised three metabolic phases characterized by different fermentation products. The bacterial community dynamics correlated with the production of the respective metabolites. In phase 1, lactic and acetic acid fermentations dominated. Accordingly, bacteria of the genera *Lactobacillus* and *Acetobacter* were detected. In phase 2, the metabolic pathways shifted to butyric acid fermentation, accompanied by the production of hydrogen and carbon dioxide and a dominance of the genus *Clostridium*. In phase 3, phylotypes affiliated with *Ruminococcaceae* and *Lachnospiraceae* prevailed, accompanied by the formation of caproic and acetic acids, and a high gas production rate.

Conclusions: A clostridial butyric-type fermentation was predominant in the acidogenic fermentation of maize silage, whereas propionic-type fermentation was marginal. As the metabolite composition resulting from acidogenesis affects the subsequent methanogenic performance, process control should focus on hydrolysis/acidogenesis when solid substrates are digested.

Keywords: Biogas, Anaerobic digestion, Maize silage, Hydrolysis, Acidogenesis, Solid-state fermentation, Bacterial 16S rRNA genes, T-RFLP fingerprinting

Background

Biogas, a mixture of mainly methane and carbon dioxide, is produced during the anaerobic digestion of biomass by a complex microbial network. Due to its high methane yield per hectare, maize is the most widely used energy crop in Germany for biogas production [1]. Usually, whole plants are harvested, chopped and

ensiled for conservation. Ensilage also serves as a pre-treatment measure for enhanced biogas production. The production of maize silage is a complex biochemical process, where bacteria produce a number of organic acids and alcohols from the maize plant material which is rich in carbohydrates, mainly starch, cellulose and hemicellulose. Several chemical and microbial silage additives are used to control the ensilage process and prevent undesirable kinds of silage fermentation. To stimulate the ensilage process, homofermentative and/or heterofermentative consortia or single strains of lactic acid bacteria are used. The homofermentative bacterial metabolism

* Correspondence: heike.strauber@ufz.de

¹Department of Bioenergy, UFZ – Helmholtz Centre for Environmental Research, in cooperation with the Deutsches Biomasseforschungszentrum, Torgauer Strasse 116, 04347, Leipzig, Germany

²Department of Environmental Microbiology, UFZ – Helmholtz Centre for Environmental Research, Permoserstrasse 15, 04318, Leipzig, Germany

results in the production of lactic acid, whereas the heterofermentative one produces a mixture of lactic acid, acetic acid, ethanol and carbon dioxide. The different fermentation pathways are accompanied by different losses of total solids (TS) during ensiling [2], whereas the content of volatile solids (VS) is only affected marginally [3]. The chemical composition of plant biomass modified by the ensilage process influences the subsequent anaerobic digestion process. Whereas the crude protein and crude fat contents of the substrate do not change during this treatment, the fiber content decreases to 15%, dependent on the fermentation conditions [3]. The digestion of the ensiled maize plants results in higher biogas yields as a direct effect of the decomposition of fibers compared to the untreated maize [3]. Furthermore, storage of the silage is possible for about 1 year. Within this time, properly ensiled plants can be used without any significant loss in methane production.

The biogas process comprises four stages, i.e., hydrolysis, acidogenesis, acetogenesis, and methanogenesis [4], which are catalyzed by different and specialized microorganisms. Parts of the metabolic network have been investigated on different levels to understand the key processes. The metabolic pathways involved in the final stage - the formation of methane by the archaea - have been intensively studied [5-7], whereas the preceding metabolic pathways catalyzed by different bacterial groups are less understood. One of the reasons is the lower diversity of methanogenic archaea involved in the biogas process compared to that of the various functional groups of bacteria [8,9]. Furthermore, methanogenesis is often the rate-limiting step, especially when wastewater is treated [10]. However, when solid substrates such as complex organic substances of plants are digested, the hydrolysis is the rate-limiting step [11,12]. Thus, to enhance the overall production rate in such processes, it is necessary to understand the primary degradation steps, i.e., hydrolysis and acidogenesis, for the control and optimization of the whole process. Although the use of maize as an energy crop is coming more and more under criticism for its negative effects on the agro-ecosystem, maize silage is a suitable model substrate to engineer solid-state fermentation processes and develop strategies for process control.

The hydrolysis of plant material is often inefficient under anaerobic conditions. The process occurs primarily through the activity of extracellular enzymes secreted by hydrolytic bacteria attached to polymeric substrates [13]. However, the hydrolytic bacteria do not gain any energy from this reaction. Hence, the same organisms perform the following acidogenesis steps by uptaking and fermenting the hydrolysis products. The range of products formed during this primary fermentation comprises various volatile fatty acids (VFA), alcohols, hydrogen and carbon dioxide. However, the ratios of the respective components can differ

significantly, dependent on the process conditions such as hydraulic retention time, organic loading rate, substrate concentration, temperature, and pH [14-16]. Process imbalances and overloading are often accompanied by an accumulation of propionic acid [17,18]. It is generally accepted that the propionic acid concentration should be kept below 1.5 g L^{-1} for proper process operation [19], and the ratio of propionic/acetic acid was suggested to be a sufficient indicator of a digester failure [17]. However, in rare cases, propionic acid was not a reliable indicator of process imbalances [20].

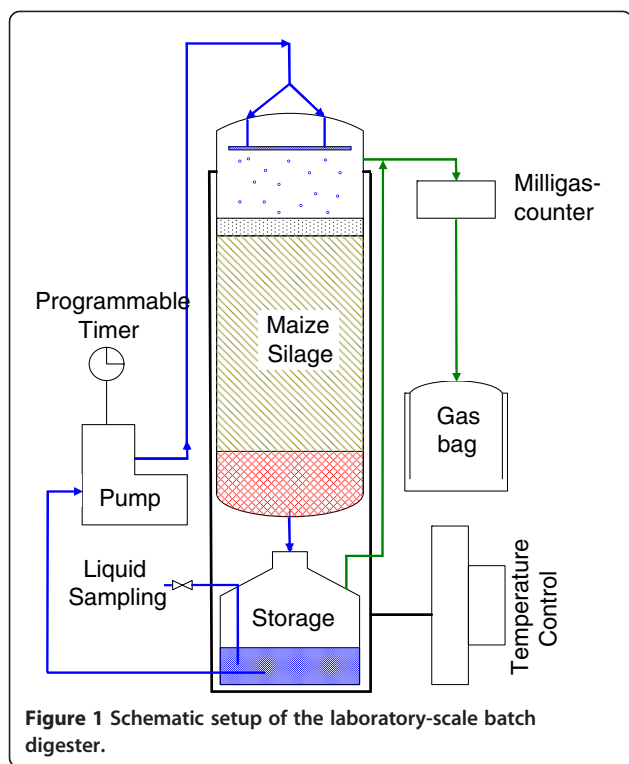
It is known that the rate of ethanol and butyric acid production accompanied by hydrogen production is relatively higher than that of propionic acid production [21]; thus, propionic acid is considered as an inferior metabolite. The metabolic background of propionic acid accumulation is not yet completely clear. Some researchers found a correlation of a high hydrogen partial pressure and an increased propionic acid production [22,23]. It is assumed that the hydrogen partial pressure regulates the metabolic reactions, as the hydrogen content determines the ratio of the oxidized NAD^+ to the reduced NADH within the bacterial cells [24]. However, the production of propionic acid was not always found to be related to a high hydrogen partial pressure, but this effect seems to be dependent on the pH value [25,26].

There are many open questions regarding the complex and functionally redundant hydrolytic and acidogenic metabolic pathways. Knowledge of the biological catalysts, i.e., the hydrolytic and fermenting bacteria, is sparse. Thus, our research is focused on the investigation of the dynamics of acidogenic fermentations, on the one hand, and the investigation of how the formation of fermentation products is reflected by the dynamics of the bacterial community composition, on the other. Correlations of the process data and the community composition have revealed both the key players involved in the process and the decisive process parameters shaping the acidogenic community. We used a solid-state leach-bed reactor as this reactor type is not only suitable for energy crops but also for more sustainable feedstocks such as straw.

Methods

Batch reactor design, operation and sampling

The hydrolysis reactor (Figure 1) was a glass column (inner diameter, 4.5 cm; total volume, 1.65 L; effective usable volume, *ca.* 1.1 L) which was heated via a water jacket at mesophilic temperatures ($37 \text{ }^\circ\text{C}$) using a water bath. Two columns (referred to as columns A and B, respectively) were run in parallel to ensure the reproducibility of the data. To each column, 200 g maize silage (TS, 41.6%_{fresh mass}; VS, 95.7%_{TS}) was spread over a polypropylene net (thickness, 2 cm) on the bottom of the column to avoid substrate discharge. A 1-cm layer of washed gravel (particle



size, 2 to 3 mm in diameter) was put onto the top of the substrate to ensure an even distribution of the percolation liquid. The digester was flushed with nitrogen to establish anoxic conditions. 500 mL anoxic tap water was used as a basis of the percolation liquid. 30 mL inoculum originating from the percolate of a previous experiment was injected to the liquid which was collected in a temperate storage tank. In this previous experiment, running under the same conditions as the experiment described here, no inoculum was used at the beginning. Prior to starting the experiment, the water/inoculum mixture was pumped in circulation over the substrate for 10 min followed by a single step for pH adjustment to an initial value of 5.46 (± 0.05) using 1 M NaOH. After that, sequential percolation (average liquid flow, 300 mL h⁻¹) was carried out throughout the whole experimental period. The hydrolysis gas was quantitatively and qualitatively analyzed as described below. The percolate was sampled once or twice a day and analyzed for pH, concentration of VFA and lactic acid, as well as for the composition of the bacterial community by terminal restriction fragment length polymorphism (T-RFLP) fingerprinting of 16S rRNA genes (see below). The pH values of the samples were measured using a pH-211 pH meter (Hanna Instruments, RI, USA). The sample was centrifuged for 2 min at 20817-g (Eppendorf Centrifuge 5417R, NY, USA), and the pellet was washed in phosphate-buffered saline and frozen at -20 °C until DNA extraction. The supernatant was used for chemical analyses. The solid

material was analyzed before and after digestion for 8 days with respect to TS and VS, nitrogen content and matrix fractions, applying the extended Weende forage analysis.

Analysis of process parameters and calculations

To determine the TS and VS contents of the substrate or the solid digestate, respectively, samples were dried at 105 °C for at least 12 h. The TS value was calculated from the difference in the weight of the fresh and the cooled, dried sample. The VS value was measured as the loss of ignition when treating the dried samples in a muffle furnace at 550 °C for 2 h. The VS value was calculated from the difference of the weight between the dried and the incinerated sample.

Total Kjeldahl nitrogen (TKN), crude protein, crude lipids, nitrogen-free extractive (NfE), cellulose and hemicellulose content of the substrate and the solid digestate were determined according to the standard procedures [27,28]. The degrees of conversion (in %) were determined for the components TS, VS, TKN, crude protein, crude lipids, NfE, cellulose, or hemicellulose of solid material. It was calculated from the absolute masses of the distinct component in the column, the substrate and the solid digestate after 8 days of fermentation using the equation below:

$$\text{Degree of conversion} = \frac{m_{sc} - m_{dc}}{m_{sc}} \times 100\%$$

where m_{sc} is the mass of the component in the substrate (in grams), and m_{dc} is the mass of the component in the solid digestate (in grams).

The concentrations of VFA (acetic, propionic, *n*-butyric, *iso*-butyric, *n*-valeric, *iso*-valeric and caproic acids) in the percolate were determined using a 5890 series II gas chromatograph (Hewlett Packard Company, CA, USA) equipped with an HS40 automatic headspace sampler (Perkin Elmer, MA, USA), an HP-FFAP column (film thickness, 0.25 μm ; inside diameter, 0.32 mm; length, 30 m; Agilent Technologies, Inc. CA, USA) and a flame ionization detector. Nitrogen was the carrier gas with a flow rate of 29 mL min⁻¹. The chromatographic conditions were as follows: injector temperature, 220 °C (split/splitless); detector temperature, 250 °C; and an oven temperature program initiating at 60 °C, followed by three sequenced temperature increases (i) at a rate of 20 K min⁻¹ up to 100 °C, (ii) 5 K min⁻¹ up to 140 °C and, finally, (iii) 40 K min⁻¹ until 200 °C was reached. One milliliter of the supernatant of a liquid sample was diluted 1:3 in distilled water (final volume, 3 mL) and filled into a 20-mL glass vial. 500 μL of 42.5% phosphoric acid and 100 μL internal standard (2-ethylbutyric acid) were added to each vial. The vials were incubated for 35 min at 80 °C before injection.

Lactic acid was analyzed using a high-performance liquid chromatograph (Shimadzu Corporation, Nakagyo-ku, Kyoto, Japan) equipped with a refractive index detector RID-6A and a Nukleogel ION 300 OA column with a pre-column (Macherey-Nagel GmbH & Co. KG, Düren, Germany). The oven temperature was 70 °C. Sulfuric acid (0.01 N) was used as the liquid phase at a flow rate of 0.6 mL min⁻¹. Liquid samples of the percolate were centrifuged (10 min at 10,000-g and 10 °C), and the supernatant was filtered using syringe filter units with cellulose acetate membranes (0.2 µm in pore size) before measurement.

Milligascounters MGC-1 V3.0 (Ritter Apparatebau GmbH and Co., Bochum, Germany) were used for the determination of the volume of the hydrolysis gas produced during the batch process. The gas amounts were monitored every day. The hydrolysis gas produced during the last 5 days was collected in gastight bags (produced on-site using thermoplastic coated aluminum foil) and analyzed in duplicate regarding H₂, N₂ and CO₂ at the end of the batch experiments. For the measurement, an HP 5890 Series II gas chromatograph (Hewlett Packard) equipped with a thermal conductivity detector and a Caboxen-1000 column (length, 4.57 m; inner diameter, 2.1 mm; Supelco, Sigma-Aldrich Corporation, MO, USA) was employed. Helium served as the carrier gas at a constant pressure of 105 kPa. The chromatographic conditions were as follows: detector temperature, 220 °C; injector temperature, 180 °C (split/splitless) and an oven temperature program starting with 5 min at 45 °C, followed by a temperature increase at a rate of 20 K min⁻¹ up to 225 °C, and this temperature was then kept for 10.5 min. The gas sample was filled into a 280-µL loop by connecting the gas bags to the gas chromatograph before injection. All three gasses were detected in significant amounts. Since nitrogen was used as a cover gas in the reactor to ensure anoxic conditions and was not microbially produced during the process, the detected concentrations of hydrogen plus carbon dioxide were set to 100%.

Molecular community analysis

Total DNA was extracted from frozen cell pellets using a FastDNA[®] SPIN Kit for soil (MP Biomedicals LLC, Illkirch, France). DNA quantity and purity were determined photometrically using a NanoDrop[®] ND-1000 UV-Vis spectral photometer (Thermo Fisher Scientific Inc., MA, USA) and by agarose gel electrophoresis. Bacterial 16S rRNA gene fragments were polymerase chain reaction (PCR)-amplified using the primers 27F and 1492R [29], and cloned as described previously [9]. Screening of the clone library, partial sequencing of representative clones and sequence analysis were performed as described by Ziganshin et al. [9]. The BLASTN tool [30,31] was used to search for

similar sequences in the GenBank database, and the RDP Classifier [32,33] was used for taxonomic assignment. The determined 16S rRNA gene sequences were deposited in the GenBank database under the accession numbers JX099788-JX099852.

For community profiling using the T-RFLP, the forward primer 27F was labeled at the 5'-end with 6-carboxyfluorescein (FAM). PCR products were purified using SureClean (Bioline GmbH, Luckenwalde, Germany) and quantified after gel electrophoresis using the GeneTools program (Syngene, Cambridge, UK). The purified PCR products were then digested with the restriction endonucleases *MseI* or *MspI*, respectively (New England Biolabs, MA, USA), using 10 U of the respective enzyme for digesting 10 ng PCR product. The samples were incubated at 37 °C overnight and then precipitated with 0.1 volumes of 3 M sodium acetate (pH 5.5) and 2.5 volumes of absolute ethanol. The dried DNA samples were resuspended in 20 µL HiDi formamide (Applied Biosystems, Life Technologies Corporation, CA, USA) containing 1.5% (v/v) MapMarker[®] 1000 (BioVentures Inc., TN, USA) labeled with 5-carboxy-X-rhodamine. The samples were denatured at 95 °C for 5 min and chilled on ice. The fragments were separated by means of capillary electrophoresis on an ABI PRISM 3130xl Genetic Analyzer (Applied Biosystems). The lengths of the fluorescent terminal restriction fragments (T-RFs) were determined using the GeneMapper V3.7 software (Applied Biosystems). The fluorescence signals of T-RFs in the range of 50 to 1,000 bp were extracted. Noise removal, peak binning to account for inter-run differences in T-RF size and normalization of signal intensity were performed using an R script (R version 2.12.2; [34]) according to [35]. The relative peak areas were determined by dividing the individual T-RF area by the total area of peaks within the range of 50 to 1,000 bp. The theoretical T-RF values of the representative phylotypes represented in the clone library were calculated using the NEB cutter [36] and confirmed experimentally by T-RFLP analysis using the corresponding clones as templates. The relative T-RF abundances of the representative phylotypes were determined based on the relative peak areas of the corresponding T-RF.

Statistical analysis

A multivariate statistical analysis of the normalized sample-peak tables was performed by means of the R package 'vegan' [37]. Non-metric multidimensional scaling (NMDS) analyses applying the Bray-Curtis similarity index (regarding the presence and relative abundance of T-RFs) were used to plot the rank order of similarity of T-RFLP profiles in a way that allows distances to be exactly expressed on a two-dimensional sheet (greater distances represent greater dissimilarities). The major process parameters correlating with the community composition as well as with single T-RFs were fitted

using the 'envfit' algorithm provided with the 'vegan' package. The significance of single process parameters for the NMDS results was tested by means of a Monte Carlo test with 1,000 permutations.

Results and discussion

The anaerobic digestion of maize silage in a solid-state fermentation reactor with percolation was monitored for 8 days. In the following, the results of column A are shown, whereas the results of the replicate batch process (column B) are presented as additional files. The results of partial sequencing of cloned 16S rRNA amplicons and the corresponding T-RF values are listed in Additional file 1.

During the anaerobic digestion, no methane production was observed indicating that only hydrolytic and acidogenic processes were active. This conclusion was confirmed by monitoring the pH value during the experimental period (Figure 2) being invariably in the acidic range between 4.8 and 6.6. Fluctuations in the pH values resulted from the degradation and production of different organic acids as described below. Similar pH values were observed during the acidogenic fermentation of both easily hydrolyzable carbohydrates in wastewater [38] or energy crops [39]. No alkalinity-producing agents were added to control the pH level during fermentation because, in most practical circumstances, the high cost of alkalis needed to maintain a high pH value during acidogenic fermentation would be prohibitive.

Concentrations of soluble substrate components and soluble and gaseous fermentation products are shown in Figure 3a and Additional file 2a. Parallel to the analytical measurements, the composition of the bacterial community was monitored by T-RFLP fingerprinting of the cells harvested from the percolate. T-RFLP profiles produced by means of the restriction enzyme *MspI* are shown in

Figure 3b and Additional file 2b, whereas the T-RFLP profiles produced by means of *MseI* are included in Additional file 3 for column A and Additional file 4 for column B. The dynamics of the T-RFLP profiles and their correlation with process parameters are visualized in an NMDS plot shown in Figure 4. During the experimental period, three different metabolic phases (phases 1, 2 and 3) indicated in Figure 3 were identified, which were characterized by the occurrence of distinct metabolites and the corresponding community dynamics. The phases were linked by interphases (1st interphase between phases 1 and 2; 2nd interphase between phases 2 and 3) shown as gray columns in Figure 3. Accordingly, the NMDS plot demonstrated that strong community shifts had occurred during the experimental time frame and that the T-RFLP profiles were clustered according to the three phases as indicated by green hulls in Figure 4. The community composition most significantly correlates with the formation of lactic acid and the VFA propionic, *n*-butyric, *iso*-butyric, *n*-valeric and *iso*-valeric acids, as well as with gas production as indicated by the vectors visualized as blue arrows in the NMDS plot.

During the first 2 days of fermentation (phase 1), acetic and lactic acids were found to be the main constituents of the percolate. Both substances originated from the respective substrate in considerable concentrations (lactic acid, about 5.3 g L^{-1} ; acetic acid, about 1.2 g L^{-1} ; both substance concentrations measured in the percolate). These organic acids are typical products of the ensilage procedure. In phase 1, the characteristic fermentation processes of the ensiling continued as both substances increased in their concentrations. Bacterial communities catalyzing the ensilage process are expected to be predominated by lactic acid-producing bacteria. Accordingly, phylotypes affiliated to the genus *Lactobacillus* were detected

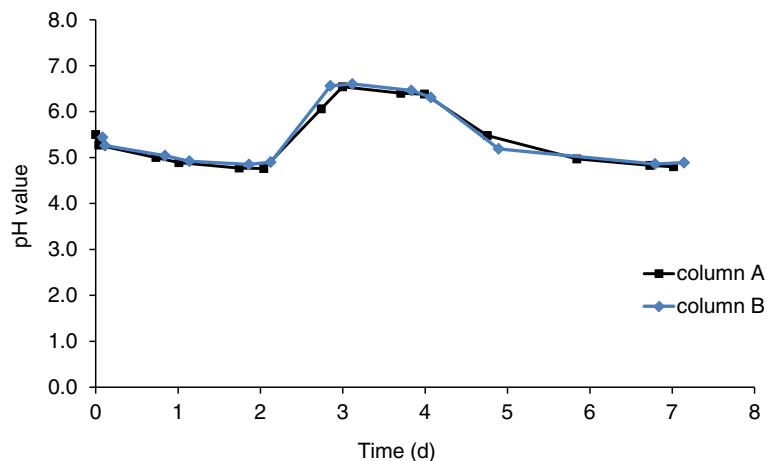
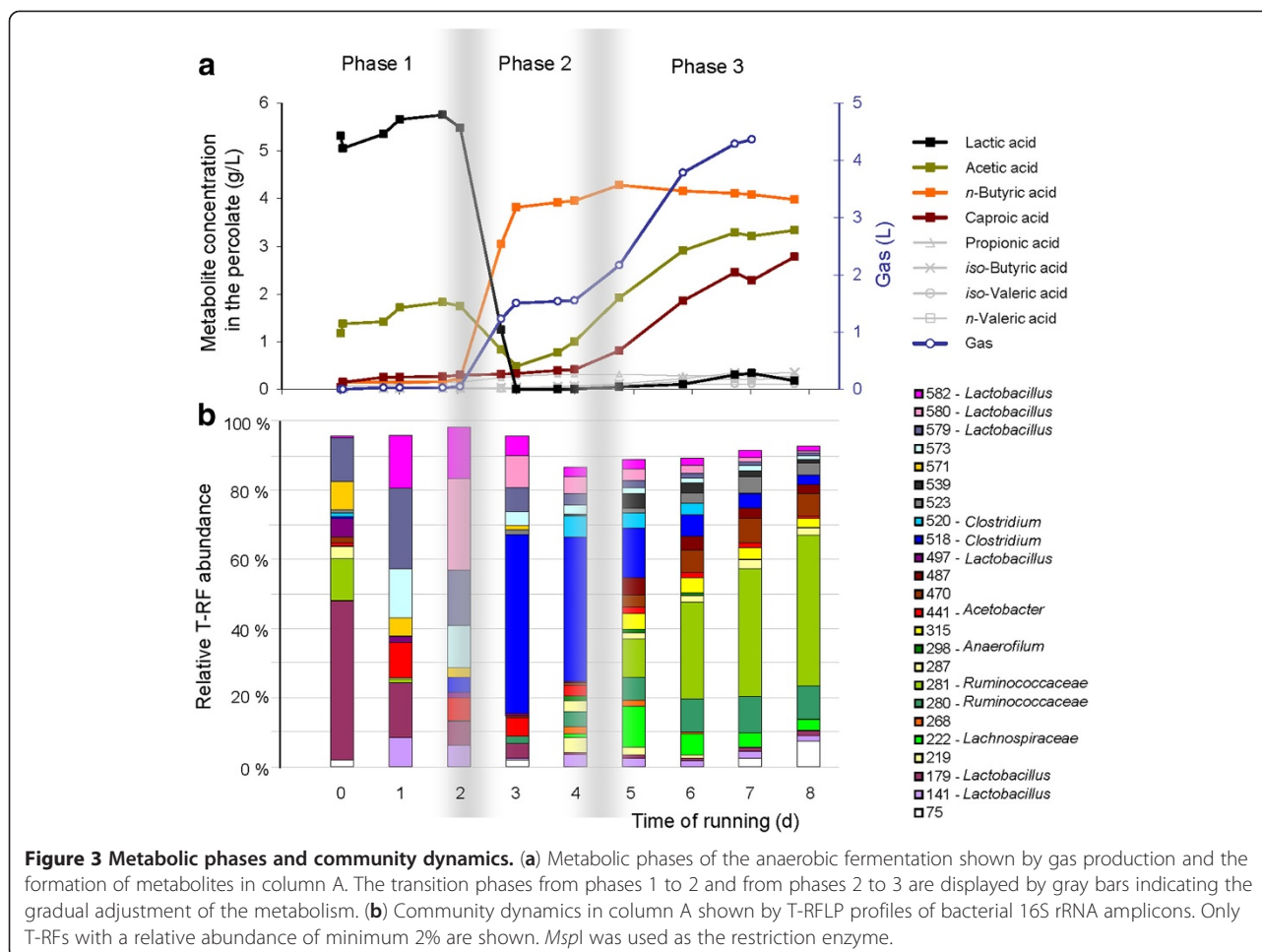


Figure 2 Time courses of the pH values in the percolates during the experimental period.



at the beginning of the acidogenic fermentation (Figure 3b, day 0). *Lactobacilli* produce lactic acid as the major fermentation product from sugars [40]. They belong to the *Firmicutes* and have a high acid tolerance, surviving pH values of 5 and lower. Therefore, they have a selective advantage over the other more acid-sensitive bacteria. As presented in Figure 4, the transition phase during the first day of fermentation (from inoculation to day 1) was characterized by a significant correlation of the community composition with the lactic acid concentration and the occurrence of several *Lactobacillus* spp. represented by the T-RFs 179, 497, 571 and 579. During the acidogenic fermentation, the bacteria continued the ensilage by producing a slightly higher concentration of both lactic and acetic acids during the first 2 days of fermentation (Figure 3a). Concomitantly, the community composition changed to the dominance of other *Lactobacillus* phylotypes, favored by the current fermentation conditions and members of the genus *Acetobacter* until day 2 (Figure 3b). *Acetobacter* species are *Alphaproteobacteria* forming acetic acid under aerobic conditions, indicating that oxygen was still present in the system. Despite becoming

overgrown by other bacteria, both the *Lactobacillus* and the *Acetobacter* related phylotypes remained present in minor proportions during the entire experimental time. This might be explained by the fact that the community composition was analyzed based on DNA, which does not necessarily reflect the actual activity of the organisms. However, based on the community shifts and the increase of other community members, the strong community dynamics became obvious.

After phase 1 during the 1st interphase, the metabolic performance of the system changed. Lactic and acetic acids were no longer produced but consumed in the 1st interphase and at the beginning of phase 2, whereas, simultaneously, butyric acid and hydrolysis gas were produced at a high rate (Figure 3a). As soon as the lactic acid was depleted, production rates of gas and butyric acid decreased drastically, pointing to a direct correlation of lactic acid degradation and butyric acid production. The production of acetic acid started again during phase 2, and the concentration of caproic acid increased slowly. The altered community composition reflected these metabolic shifts between phases 1 and 2 (Figure 3b). After day 3, the

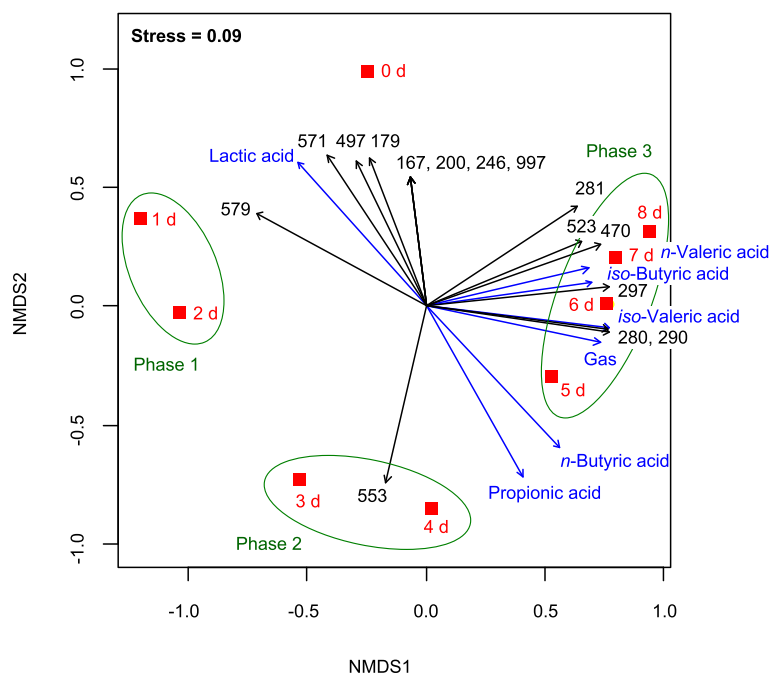


Figure 4 NMDS analysis plot. T-RFLP profiles of bacterial 16S rRNA amplicons digested with the restriction enzyme *MspI* (column A). Sampling times are indicated by red squares. Community similarity is based on the Bray-Curtis index which includes the presence and relative abundance of T-RFs. Blue arrows indicate the correlation vectors of community differences and the process parameters with significance factors $p < 0.05$. Black arrows indicate the correlation vectors of single T-RFs and the process parameters with significance factors $p < 0.01$. Significance was tested by Monte-Carlo permutation against 999 random data sets. Green hulls indicate the three metabolic phases of the batch experiment (see Figure 3).

Lactobacillus and *Acetobacter* strains were gradually replaced by phylotypes affiliated to the genus *Clostridium*. The clostridial phylotype with the T-RF 518, which emerged on day 2, became the dominant community member on days 3 and 4. The clostridia are strict anaerobes and represent one of the most prevalent bacterial groups in biogas reactors. *C. thermocellum* and *C. stercorarium* were identified as the major players in the hydrolysis of plant biomass [41], whereas *C. thermopalmarium* was found to be the main butyric acid producer in a wastewater treatment system [42]. The clostridia represent the majority of the light-independent fermentative bacteria which have the ability to produce hydrogen [43].

In the 2nd interphase between phases 2 and 3, the formation of fermentation products accelerated. Hydrolysis gas as well as acetic and caproic acids were produced, whereas the concentration of butyric acid increased only marginally (Figure 3a). During phase 3, this metabolic behavior continued as reflected by significantly increased concentrations of acetic and caproic acids, accompanied by a comparably high gas production rate of up to 1.5 L d⁻¹. However, butyric acid production decreased slowly. On day 6, lactic acid was produced again in minor amounts but degraded during the following day, reflecting the ongoing dynamics of the fermentation process. The community composition on day 6 was most significantly

correlated with gas production and formation of *iso*-valeric acid, whereas on day 7, a significant correlation with *iso*-butyric and *n*-valeric acid concentrations was visible (Figure 4). During the 2nd interphase, the *Clostridium* strains represented by the T-RFs 518 and 520 were overgrown by phylotypes affiliated to the *Ruminococcaceae* and *Lachnospiraceae* (Figure 3b). As shown in Figure 4, the decisive phylotype correlated with day 6 was T-RF 280 which represents a member of the *Ruminococcaceae*. The *Ruminococcaceae* and *Lachnospiraceae* belong to the order *Clostridiales*. The *Ruminococcaceae* can hydrolyze a variety of polysaccharides by different mechanisms, e.g., the production of a cellulosome enzyme complex and cellulose adhesion proteins [44]. Moreover, they are able to ferment hexoses as well as pentoses. The production of hydrogen by *Ruminococcus albus* from sweet sorghum was reported by Ntaikou et al. [45]. Various genera of *Lachnospiraceae* are known to produce large amounts of *n*-butyric acid, acetic acid and carbon dioxide through the fermentation of carbohydrates [46].

At the end of the acidogenic batch fermentation, a VFA concentration of 11.24 g L⁻¹ was achieved, consisting of 3.34 g L⁻¹ acetic acid, 0.28 g L⁻¹ propionic acid, 0.36 g L⁻¹ *iso*-butyric acid, 3.98 g L⁻¹ *n*-butyric acid, 0.11 g L⁻¹ *iso*-valeric acid, 0.24 g L⁻¹ *n*-valeric acid, 2.77 g L⁻¹ caproic acid, and 0.18 g L⁻¹ lactic acid. In

total, 4.37 L hydrolysis gas composed of 35.2% hydrogen and 68.8% carbon dioxide was produced.

The VS content of 38.2%_{fresh mass} in the substrate was diminished to 18.6%_{fresh mass} in the solid digestate. This corresponds to a degree of degradation of 44% within 8 days of acidogenic fermentation (Table 1). Maize silage is a feedstock rich in carbohydrates as reflected by the predominating fraction of NfEs in the Weende forage analysis. The detailed analysis of the substrate and the digestate compounds revealed a consistent degradation of the crude protein, hemicellulose and NfE fractions (Table 1). The crude lipid fraction was converted to a slightly lower proportion, and only 11% of the cellulose fraction was used as a substrate for fermentation. In maize plants, the hemicellulose and cellulose fiber materials form a complex together with lignin known as lignocellulose. As lignin is not degradable by bacterial attack under anaerobic conditions, it diminishes the bio-availability of the hydrolyzable compounds cellulose and hemicellulose. During the acidogenic fermentation of maize silage, we observed the preferential degradation of hemicellulose compared to cellulose being the result of the higher accessibility of hemicellulose for bacteria, as hemicellulose restricts the access to the crystalline cellulose cores of the microfibrils by coating them [47].

A mixture of acetic, *n*-butyric, caproic and lactic acids developed as metabolites which are characteristic of clostridial fermentation. Propionic, *iso*-butyric and *n*-valeric acids were produced only in minor amounts. This result indicates that butyric-type fermentation was dominant, whereas propionic-type fermentation characterized by the production of propionic, acetic and some valeric acids

without a significant gas production [48] was marginal. Lactic acid was observed to be an intermediate fermentation product as it was firstly produced and subsequently metabolized during the process. This type of fermentation is certainly a characteristic of the digestion of silages, as active lactic acid producing bacterial strains are inoculated in a considerable amount along with the substrate. However, the appearance of lactic acid was also observed with other carbohydrate-rich substrates [49] and garbage [50].

The performance of the acidogenic fermentation strongly depends on the process conditions. Contradictory results were reported regarding the effect of the pH on the product composition, which was shown to be negligible in the range of 5 to 7 [38,51], while other researchers detected a pronounced influence [15,16,26,52,53]. Veeken et al. [54] observed that the hydrolysis rate during the anaerobic digestion of organic solid waste was not related to the total or undissociated VFA concentrations but was found to be pH dependent. The cellulase system of *C. thermocellum* works with a smaller hydrolysis rate at pH values below 6.5 [41]. Most of the studies were carried out using wastewater treatment systems. Therefore, little is known about the pH impact on the acidogenic fermentation of energy crops and the molecular mechanisms of pH effects. Evidently, different pH optima do not exist for metabolic pathways but for the microorganisms which carry out these reactions. They do not only catalyze the desired fermentations but also grow by increasing cell size and performing cell divisions at a species-specific rate. The composition of an operating bacterial community is determined by the composition of the inoculum. Depending on the environmental conditions and the distinct sensitivities of the persisting bacteria, the community will develop.

The composition of the bacterial products of the acidogenic fermentation determines the rates and performance of the subsequent metabolic steps, i.e., acetogenesis and methanogenesis. Acetic acid can directly be used by the acetoclastic methanogens for biogas production. In single-stage biogas processes, all metabolic steps occur in one reactor simultaneously. Organic acids are detected as intermediate products only in minor amounts, and the accumulation of VFA and the lowering of the pH are known to lead to the suppression of the methanogenic activity and to a process failure in single-stage reactors. Two-stage processes are characterized by separated hydrolysis/acidogenesis and acetogenesis/methanogenesis [55]. Numerous advantages of two-stage processes over the conventional biogas production have been described [55,56]. These include increased process stability, control and efficiency, as well as a high tolerance to overloading. In two-stage processes, the production of bio-products (VFA or lactic acid) for industrial use and biogas for covering energy demands can be combined [49,53,57]. In such systems and other reactors with separate hydrolysis, e.g., plug-flow

Table 1 Extended Weende forage analysis of maize silage and solid digestate after 8 days of acidogenic fermentation

Parameter	Substrate	Solid digestate	Degree of conversion (%)
Fresh mass (g)	200	230	
TS (% _{fresh mass})	40.0	20.2	42
VS (% _{fresh mass})	38.2	18.6	44
TKN (g/kg _{TS})	10.3	8.9	50
Crude protein (g/kg _{TS})	64.2	55.9	49
Crude lipid (g/kg _{TS})	25.9	26.4	41
NfE, including starch (g/kg _{TS})	659.6	532.6	53
Cellulose (g/kg _{TS})	185.7	283.5	11
Hemicellulose (g/kg _{TS})	385.5	356.2	46

TS, total solids; VS, volatile solids; TKN, total Kjeldahl nitrogen; NfE, nitrogen-free extractive. The degrees of conversion were calculated as described in the methods section.

reactors, the control of the acidogenic reactions is of special interest, as different metabolite compositions lead to a different methanogenic performance. For example, the rate of butyric acid conversion has been found to be higher than that of the other VFA [58]. Propionic acid degradation is largely inhibited during periods of high activity of the butyric acid-converting bacteria, whereas acetic acid exerts a weaker influence on the conversion of propionic acid [59]. However, high activity single-stage fermenters are commonly used in the biogas industry. In these full-scale reactors, high-performance hydrolysis and optimal methanogenesis do not exclude each other when running in parallel within one reactor. Nevertheless, further research could help in the engineering of the first phase with the objective of obtaining desirable fermentation products and enhanced biogas production rates.

Conclusions

Batch acidogenic fermentation of maize silage occurs in three metabolic phases characterized by the production of distinct primary fermentation products and correlating with the respective bacterial key players. The clostridial butyric-type fermentation predominates, whereas the propionic-type fermentation is marginal. The composition of the inoculum seems to influence the performance of the hydrolysis and acidogenesis steps. Further studies should reveal the metabolic dynamics and community composition when using both a continuous fermentation regime and solid substrates other than maize silage.

As the metabolite composition of the acidogenesis affects the subsequent methanogenic performance, process control and optimization should focus on the first two phases, i.e., hydrolysis and acidogenesis of the biogas production when solid substrates are digested. Especially in plug-flow digesters or digesters with a separated hydrolysis (two-stage systems), the control of the acidogenic reactions is important. More detailed analyses of the hydrolysis and acidogenesis steps in solid-state fermentation are needed for the efficient exploitation of more sustainable feedstocks such as straw or energy crops other than maize.

Additional files

Additional file 1: Title: Sequencing results of representative bacterial 16S rRNA gene clones and theoretically/experimentally determined terminal restriction fragments (T-RFs). **Description:** Clone libraries were generated from the samples of column B (23 = 2 d, 25 = 4 d, 27 = 6 d, 31 = 0 d). For BLAST comparison, the sequences from uncultured clones were excluded. Taxonomic assignment is based on RDP Classifier results at 50% confidence threshold.

Additional file 2: Title: (a) Metabolic phases and community dynamics in column B. **Description:** Metabolic phases of the anaerobic fermentation shown by gas production and the formation of metabolites in column B. The transition phases from phase 1 to phase 2 and from phase 2 to phase 3 are displayed by gray bars indicating the gradual adjustment of the metabolism. (b) Community dynamics in column B is shown

by T-RFLP profiles of bacterial 16S rRNA amplicons. Only T-RFs with a relative abundance of minimum 2% are presented. *MspI* was used as a restriction enzyme.

Additional file 3: Title: Community dynamics in column A according to restriction analysis with *MseI*. **Description:** T-RFLP profiles of bacterial 16S rRNA amplicons retrieved from column A. Only T-RFs with a relative abundance of minimum 2% are presented.

Additional file 4: Title: Community dynamics in column B according to restriction analysis with *MseI*. **Description:** T-RFLP profiles of bacterial 16S rRNA amplicons retrieved from column B. Only T-RFs with a relative abundance of minimum 2% are presented.

Abbreviations

NfE: nitrogen-free extractives; NMDS: non-metric multidimensional scaling; PCR: polymerase chain reaction; TKN: total Kjeldahl nitrogen content; T-RF: terminal restriction fragment; T-RFLP: terminal restriction fragment length polymorphism; TS: total solids; VFA: volatile fatty acids; VS: volatile solids.

Competing interests

The authors declare that they have no competing interests.

Acknowledgments

This work was supported by the Initiative and Networking Fund of the Helmholtz Association. We would like to thank our collaboration partners from the Department of Biochemical Conversion of the Deutsches Biomasseforschungszentrum (DBFZ) for contributing to the analytical measurements. Furthermore, we would like to thank Ute Lohse for her technical assistance with molecular analyses.

Authors' contributions

HS carried out the bioreactor experiments and analytics, and wrote the manuscript. MS performed the experimental work for the community analyses and contributed to T-RFLP and sequence data analyses. SK carried out the phylogenetic and the statistical analyses, and contributed to the writing of the manuscript. HS and SK conceived of the study and participated in its design and coordination. All authors read and approved the final manuscript.

Dedication

This publication is dedicated to Prof. Wolfgang Babel on the occasion of his 75th birthday.

Received: 26 June 2012 Accepted: 16 July 2012

Published: 16 July 2012

References

1. Amon T, Amon B, Kryvoruchko V, Zollitsch W, Mayer K, Gruber L (2007) Biogas production from maize and dairy cattle manure—influence of biomass composition on the methane yield. *Agr Ecosyst Environ* 118:173–182.
2. McDonald P, Henderson AR, Heron SJE (1991) *The biochemistry of silage*, 2nd edn. Chalcombe Publications, Marlow, England.
3. Herrmann C, Heiermann M, Idler C (2011) Effects of ensiling, silage additives and storage period on methane formation of biogas crops. *Bioresour Technol* 102:5153–5161.
4. Lynd LR, Weimer PJ, van Zyl WH, Pretorius IS (2002) Microbial cellulose utilization: fundamentals and biotechnology. *Microbiol Mol Biol Rev* 66(3):506–577.
5. Demirel B, Scherer P (2008) The roles of acetotrophic and hydrogenotrophic methanogens during anaerobic conversion of biomass to methane: a review. *Rev Environ Sci Biotechnol* 7:173–190.
6. Narihiro T, Sekiguchi Y (2008) Microbial communities in anaerobic digestion processes for waste and wastewater treatment: a microbiological update. *Curr Opin Biotechnol* 18:273–278.
7. Weiland P (2010) Biogas production: current state and perspectives. *Appl Microbiol Biotechnol* 85:849–860.
8. Cardinali-Rezende J, Debarry RB, Colturato LFDB, Carneiro EV, Chartone-Souza E, Nascimento AMA (2009) Molecular identification and dynamics of microbial communities in reactor treating organic household waste. *Appl Microbiol Biotechnol* 84:777–789.

9. Ziganshin AM, Schmidt T, Scholwin F, Il'inskaya ON, Harms H, Kleinstüber S (2011) Bacteria and archaea involved in anaerobic digestion of distillers grains with solubles. *Appl Microbiol Biotechnol* 89:2039–2052.
10. Pavlostathis SG, Giraldo-Gomez E (1991) Kinetics of anaerobic treatment: a critical review. *Crit Rev Environ Contr* 21(5,6):411–490.
11. Noike T, Endo G, Chang J, Yaguchi J, Matsumoto J (1995) Characteristics of carbohydrate degradation and the rate-limiting step in anaerobic digestion. *Biotechnol Bioeng* 27:1482–1489.
12. Mata-Alvarez J, Macé S, Labrés P (2000) Anaerobic digestion of organic solid wastes. An overview of research achievements and perspectives. *Bioresour Technol* 74:3–16.
13. Song H, Clarke WP, Blackall LL (2005) Concurrent microscopic observations and activity measurements of cellulose hydrolyzing and methanogenic populations during the batch anaerobic digestion of crystalline cellulose. *Biotechnol Bioeng* 91(3):369–378.
14. De la Torre I, Goma G (1981) Characterization of anaerobic microbial culture with high acidogenic activity. *Biotechnol Bioeng* 23:185–199.
15. Breure AM, van Andel JG (1984) Hydrolysis and acidogenic fermentation of a protein, gelatin, in an anaerobic continuous culture. *Appl Microbiol Biotechnol* 20:40–45.
16. Dinopoulou G, Rudd T, Lester JN (1988) Anaerobic acidogenesis of a complex wastewater: 1. The influence of operational parameters on reactor performance. *Biotechnol Bioeng* 31:958–968.
17. Marchaim U, Krause C (1993) Propionic to acetic acid ratios in overloaded anaerobic digestion. *Bioresour Technol* 43:195–203.
18. Wang L, Zhou Q, Li FT (2006) Avoiding propionic acid accumulation in the anaerobic process for biohydrogen production. *Biomass Bioenergy* 30:177–182.
19. Ma J, Carballa M, Van de Caveyea P, Verstraete W (2009) Enhanced propionic acid degradation (EPAD) system: proof of principle and feasibility. *Water Res* 43:3239–3248.
20. Leuhn M, Liu F, Heuwwinkel H, Gronauer A (2008) Biogas production from mono-digestion of maize silage – long-term process stability and requirements. *Water Sci Technol* 58(8):1645–1651.
21. Hanaki K, Hirunmasuwan S, Matsuoto T (1994) Selective use of microorganisms in anaerobic treatment processes by application of immobilization. *Water Res* 28(4):993–996.
22. Harper SR, Pohland FG (1986) Recent developments in hydrogen management during anaerobic biological wastewater treatment. *Biotechnol Bioeng* 28:585–602.
23. Mosey FE, Fernandes XA (1989) Patterns of hydrogen in biogas from the anaerobic digestion of milk-sugars. *Water Sci Technol* 21:187–196.
24. Mosey FE (1983) Mathematical modelling of the anaerobic digestion process: Regulatory mechanisms for the formation of short-chain volatile acids from glucose. *Water Sci Technol* 15:209–232.
25. Inanc B, Matsui S, Ide S (1996) Propionic acid accumulation and controlling factors in anaerobic treatment of carbohydrate: effects of H₂ and pH. *Water Sci Technol* 34(5–6):317–325.
26. Ren N, Wang B, Huang J-C (1997) Ethanol-type fermentation from carbohydrate in high rate acidogenic reactor. *Biotech Bioeng* 54(5):428–433.
27. Naumann C, Bassler R (2006) VDLUFA Methodenbuch: Die Chemische Untersuchung von Futtermitteln. Band III, VDLUFA-Verlag, Darmstadt.
28. Van Soest PJ, Robertson JB, Lewis BA (1991) Methods for dietary fiber, neutral detergent fiber, and nonstarch polysaccharides in relation to animal nutrition. *J Dairy Sci* 74:3583–3597.
29. Lane DJ (1991) 16S/23S rRNA sequencing. In: Stackebrandt E, Goodfellow M (eds) *Nucleic acid techniques in bacterial systematics*. John Wiley & Sons, Chichester, pp 177–203.
30. Basic Local Alignment Search Tool (2009), The BLASTN tool. www.ncbi.nlm.nih.gov/BLAST. Accessed April 24, 2012.
31. Altschul SF, Gish W, Miller W, Myers EW, Lipman DJ (1990) Basic local alignment search tool. *J Mol Biol* 215:403–410.
32. Michigan State University (2011) The RDP Classifier. <http://rdp.cme.msu.edu>. Accessed April 24, 2012.
33. Wang Q, Garrity GM, Tiedje JM, Cole JR (2007) Naive Bayesian classifier for rapid assignment of rRNA sequences into the new bacterial taxonomy. *Appl Environ Microbiol* 73:5261–5267.
34. R Development Core Team (2009) R: a language and environment for statistical computing. R Foundation for Statistical Computing, Vienna, Austria, p ISBN 3-900051-07-0. <http://www.R-project.org>. Accessed April 20, 2012.
35. Abdo Z, Schuette UM, Bent SJ, Williams CJ, Forney LJ, Joyce P (2006) Statistical methods for characterizing diversity of microbial communities by analysis of terminal restriction fragment length polymorphisms of 16S rRNA genes. *Environ Microbiol* 8:929–938.
36. New England Biolabs, Inc (2011) The NEB cutter. <http://tools.neb.com/NEBcutter2>. Accessed April 25, 2012.
37. Oksanen J (2011) Multivariate analysis of ecological communities in R: vegan tutorial., <http://cc.oulu.fi/~jarioksa/opetus/metodi/vegantutor.pdf>. Accessed April 20, 2012.
38. Zoetemeyer RJ, van den Heuvel JC, Cohen A (1982) pH influence on acidogenic dissimilation of glucose in an anaerobic digester. *Water Res* 16:303–311.
39. Zielonka S, Lemmer A, Oechsner H, Jungbluth T (2010) Energy balance of a two-phase anaerobic digestion process for energy crops. *Eng Life Sci* 10(6):515–519.
40. Stiles ME, Holzapfel WH (1997) Lactic acid bacteria of foods and their current taxonomy. *Int J Food Microbiol* 36:1–29.
41. Zverlov WW, Hiegl W, Köck DE, Kellermann J, Köllmeier T, Schwarz WH (2010) Hydrolytic bacteria in mesophilic and thermophilic degradation of plant biomass. *Eng Life Sci* 10(6):528–536.
42. Kim MD, Song M, Jo M, Shin SG, Kim JH, Hwang S (2010) Growth condition and bacterial community for maximum hydrolysis of suspended organic materials in anaerobic digestion of food waste-recycling wastewater. *Appl Microbiol Biotechnol* 85:1611–1618.
43. Das D, Veziroglu TN (2001) Hydrogen production by biological processes: a survey of literature. *Int J Hydrogen Energy* 26:13–28.
44. Morrison M, Miron J (2000) Adhesion to cellulose by *Ruminococcus albus*: a combination of cellulosomes and Pil-proteins? *FEMS Microbiol Lett* 185:109–115.
45. Ntaikou I, Gavala HN, Kornaros M, Lyberatos G (2008) Hydrogen production from sugars and sweet sorghum biomass using *Ruminococcus albus*. *Int J Hydrogen Energy* 33(4):1153–1163.
46. Cotta M, Forster R (2006) The family Lachnospiraceae, including the genera *Butyrivibrio*, *Lachnospira* and *Roseburia*. In: Dworkin M, Falkow S, Rosenberg E, Schleifer K-H, Stackebrandt E (eds) *The prokaryotes: a handbook on the biology of bacteria: Bacteria: Firmicutes, Cyanobacteria*, vol 4, 3rd edn. Springer, New York.
47. Ding SY, Himmel ME (2006) The maize primary cell wall microfibril: a new model derived from direct visualization. *J Agr Food Chem* 54(3):597–606.
48. Cohen A, van Gemert JM, Zoetemeyer RJ, Breure AM (1984) Main characteristics and stoichiometric aspects of acidogenesis of soluble carbohydrate containing wastewaters. *Process Biochem* 19(6):228–232.
49. Parawira W, Murto M, Read JS, Mattiasson B (2004) Volatile fatty acid production during anaerobic mesophilic digestion of solid potato waste. *J Chem Technol Biotechnol* 79:673–677.
50. Akao S, Tsuno H, Horie T, Mori S (2007) Effects of pH and temperature on products and bacterial community in L-lactate batch fermentation of garbage under unsterile condition. *Water Res* 41:2636–2642.
51. Joergensen MH (1978) Anaerobic formation of volatile acids in a chemostat. *European J Appl Microbiol Biotechnol* 6:181–187.
52. Kisaalita WS, Pinder KL (1987) Acidogenic fermentation of lactose. *Biotechnol Bioeng* 30:88–95.
53. Horiuchi J-I, Shimizu T, Tada K, Kanno T, Kobayashi M (2002) Selective production of organic acids in anaerobic acid reactor by pH control. *Bioresour Technol* 82:209–213.
54. Veeken A, Kalyuzhnyi S, Scharrf H, Hamelers B (2000) Effect of pH and VFA on hydrolysis of organic solid waste. *J Environ Eng-ASCE* 126(12):1076–1081.
55. Demirel B, Yenigün O (2002) Two-phase anaerobic digestion processes: a review. *J Chem Technol Biotechnol* 77:743–755.
56. Lv W, Schanbacher FL, Yu Z (2010) Putting microbes to work in sequence: recent advances in temperature-phased anaerobic digestion processes. *Bioresour Technol* 101:9409–9414.
57. Hofvendahl K, Hahn-Hägerdal B (2000) Factors affecting the fermentative lactic acid production from renewable resources. *Enzyme Microb Tech* 26:87–107.
58. Cohen A, Breure AM, van Andel JG, van Deursen A (1982) Influence of phase separation on the anaerobic digestion of glucose – II: stability, and kinetic responses to shock loadings. *Water Res* 16:449–455.
59. Wiegant WM, Hennink M, Lettinga G (1986) Separation of the propionate degradation to improve the efficiency of thermophilic anaerobic treatment of acidified wastewaters. *Water Res* 20(4):517–524.

doi:10.1186/2192-0567-2-13

Cite this article as: Sträuber et al.: Metabolic and microbial community dynamics during the hydrolytic and acidogenic fermentation in a leach-bed process. *Energy, Sustainability and Society* 2012 2:13.